



# Physical limitation of pesticides (chlordecone) decontamination in volcanic soils: fractal approach and numerical simulation

Thierry Woignier, Luc Rangon, Florence Clostre, Charles Mottes, Philippe Cattan, Juan Primera, Magalie Jannoyer

## ► To cite this version:

Thierry Woignier, Luc Rangon, Florence Clostre, Charles Mottes, Philippe Cattan, et al.. Physical limitation of pesticides (chlordecone) decontamination in volcanic soils: fractal approach and numerical simulation. *Environmental Science and Pollution Research*, 2020, 27 (33), pp.40980-40991. 10.1007/s11356-019-05899-0 . hal-02522014

**HAL Id: hal-02522014**


**<https://hal.science/hal-02522014>**

Submitted on 27 Mar 2020

**HAL** is a multi-disciplinary open access archive for the deposit and dissemination of scientific research documents, whether they are published or not. The documents may come from teaching and research institutions in France or abroad, or from public or private research centers.

L'archive ouverte pluridisciplinaire **HAL**, est destinée au dépôt et à la diffusion de documents scientifiques de niveau recherche, publiés ou non, émanant des établissements d'enseignement et de recherche français ou étrangers, des laboratoires publics ou privés.

# Physical limitation of pesticides (chlordecone) decontamination in volcanic soils: fractal approach and numerical simulation

Thierry Woignier<sup>1,2</sup>  • Luc Rangon<sup>1,2</sup> • Florence Clostre<sup>3</sup> • Charles Mottes<sup>3,4</sup> • Philippe Cattan<sup>5,6</sup> • Juan Primera<sup>7,8</sup> • Magalie Jannoyer<sup>3,4</sup>

## Abstract

In the French West Indies, the chlordecone (organochloride pesticide) pollution is now diffuse becoming new contamination source for crops and environment (water, trophic chain). Decontamination by bioremediation and chemical degradation are still under development but the physical limitations of these approaches are generally not taken into account. These physical limitations are related to the poor physical accessibility to the pesticides in soils because of the peculiar structural properties of the contaminated clays (pore volume, transport properties, permeability, and diffusion). Some volcanic soils (andosols), which represent the half of the contaminated soils in Martinique, contain nanoclay (allophane) with a unique structure and porous properties. Andosols are characterized by pore size distribution in the mesoporous range, a high specific surface area, a large pore volume, and a fractal structure. Our hypothesis is that the clay microstructure characteristics are crucial physico-chemical factors strongly limiting the remediation of the pesticide. Our results show that allophane microstructure (small pore size, hierarchical microstructure, and tortuosity) favors accumulation of chlordecone, in andosols. Moreover, the clay microporosity limits the accessibility of microorganisms and chemical species able to decontaminate because of poor transport properties (permeability and diffusion). We model the transport properties by two approaches: (1) we use a numerical model to simulate the structure of allophane aggregates. The algorithm is based on a cluster–cluster aggregation model. From the simulated data, we derived the pore volume, specific surface area, tortuosity, permeability, and diffusion. We show that transport properties strongly decrease because of the presence of allophane. (2) The fractal approach. We characterize the fractal features (size of the fractal aggregate, fractal dimension, tortuosity inside allophane aggregates) and we calculate that transport properties decrease of several order

ranges inside the clay aggregates. These poor transport properties are important parameters to explain the poor accessibility to pollutants in volcanic soils and should be taken into account by future decontamination process. We conclude that for andosols, this inaccessibility could render inefficient some of the methods proposed in the literature.

✉ Thierry Woignier  
thierry.woignier@imbe.fr

<sup>1</sup> Aix Marseille Université, Univ Avignon, CNRS, IRD, IMBE, Marseille, France

<sup>2</sup> IRD, UMR IMBE, Campus Agro-environnemental Caraïbe, Le Lamentin, Martinique, France

<sup>3</sup> Cirad, UPR HortSys, F-97285 Le Lamentin, France

<sup>4</sup> HortSys, Univ Montpellier, Cirad, Inra, Inria, Montpellier SupAgro, Montpellier, France

<sup>5</sup> CIRAD, UPR GECO, F-34398 Montpellier, France

<sup>6</sup> GECO, Univ Montpellier, CIRAD, Montpellier, France

<sup>7</sup> Facultad de Ingeniería Agrícola, Departamento de Ciencias Agrícolas, Universidad Técnica de Manabí, Lodana, Provincia de Manabí, Ecuador

<sup>8</sup> Facultad Experimental de Ciencias, Departamento de Física, Universidad del Zulia, Edo Zulia, Venezuela

**Keywords** Chlordecone · Soil contamination · Allophane clay · Andosols · Numerical simulation · Permeability · Diffusion, Fractal structure

## Introduction

The French West Indies (FWI) are affected by severe agricultural pollution by chlordecone (CLD). Chlordecone is an organochlorine molecule made of 10 atoms of carbon and chlorine and a single oxygen atom. It is a homocubane configuration of 0.53–0.65 nm size, with high steric hindrance (Durimel et al. 2013). Through this peculiar structure, chlordecone

molecule has a high stability. The CLD chemical properties are as follows: molecular mass  $490.64 \text{ g mol}^{-1}$ ; a low solubility in water, except at  $\text{pH} > 9$  (Dawson et al. 1979); a vapor tension of CLD less than  $3 \times 10^{-2} \text{ Pa}$  at  $25^\circ\text{C}$ , and the sublimation temperature is over  $350^\circ\text{C}$ . Its partitioning coefficient (Koc) between the sorbed part on soil organic matter and the dissolved part in water is high, between 2000 and 2500  $\text{L kg}^{-1}$  (ATSDR 1995). CLD is known for its neurotoxic and carcinogenic properties (Dallaire et al. 2012; Epstein 1978; Multigner et al. 2010). In 1993, CLD was prohibited in FWI (Cabidoche et al. 2009); in 2009, CLD was included in the Stockholm Convention annexes and its use was banned worldwide (UNEP 2007).

This organochlorine molecule persists in the soils of banana fields where it was applied more than 25 years ago (Brunet et al. 2009; Cabidoche et al. 2009; Lesueur Jannoyer et al. 2016; Levillain et al. 2012), and until now, no treatment has been definitively validated to remediate the situation. CLD will continue to contaminate all environmental compartments and trophic chains (soil, water, crops, animals, and thus foodstuffs) for many years (Cabidoche and Lesueur-Jannoyer 2012; Coat et al. 2011; Jondreville et al. 2013; Mottes et al. 2016, 2017; Della Rossa et al. 2017; Clostre et al. 2017). This leads to the contamination of the entire food web and the local population is thus exposed to CLD through food (Dubuisson et al. 2007) making the pollution of soils a public health concern.

In Martinique (FWI), pesticides interact with the three main types of soil: andosol, nitisol, and ferralsol. However, even if andosols are polluted at higher levels than nitisols and ferralsols (Brunet et al. 2009; Clostre et al. 2014a; Levillain et al. 2012), transfers not only from soil to plants but also from soils to water (Cabidoche et al. 2009; Woignier et al. 2015) are lower. It is widely admitted that the availability of each pesticide is related to their physical-chemical properties: solubility, chemical affinity with organic matter, and biodegradability (Pignatello 1998; Semple et al. 2001). However, the structural properties of the mineral matrix with which pesticides are associated may also influence pollutant bioavailability (Peters et al. 2007; Chung and Alexander 2002; Liu et al. 2009). The lower availability in andosols can be physically explained as the result of the pollutant entrapment (Calabi-Floody et al. 2011; Garrido-Ramirez et al. 2012).

Decontamination solutions for water and soils are under development. Gaspard and coworkers (Durimel et al. 2013; Gaspard et al. 2016) prepared activated carbons with different textural properties and surface chemistry from sugarcane bagasse (SCB ACs) to remove CLD from contaminated water.

Phytoremediation by plants is limited by the very low soil-to-plant transfer rates (Liber et al. 2018; Clostre et al. 2014b; Woignier et al. 2012).

In the literature, two main methods are under study for soils: bioremediation and ISCR (in situ chemical reduction).

It is generally accepted that natural degradation of CLD in soils is very poor (Cabidoche et al. 2009; Dolfing et al. 2012) and authors ask for the existence of thermodynamics, biological and chemical conditions to naturally degrade CLD. However, a few years ago, Macarie and coworkers (Macarie et al. 2016) show that there are no thermodynamic reasons for limiting the CLD degradation. Recently, Chevallier et al. (2019) also found metabolites of CLD (dechlorinated CLD derivatives with loss of up to 7 Cl) in Caribbean soils. They also show that microorganisms, susceptible to degrade CLD, are present in the Caribbean soils demonstrating that natural biodegradation should be possible. One of the open questions is why the natural degradation is so poor.

The principle of ISCR is coupling zero valent iron (ZVI) with an organic amendment, leading to chemical reduction and stimulation of bacterial activity (Mouvet et al. 2016). ISCR is a proved technique used for the decontamination of PCBs (Irwin Abbey et al. 2003), lindane hexachlorocyclohexane (Phillips et al. 2006), toxaphene ( $\text{C}_{10}\text{Cl}_{18}\text{H}_{10}$ ) (Seech et al. 2008), and metolachlore (Kim et al. 2010). In the case of CLD, this method has shown encouraging results in laboratory (Mouvet et al. 2016) and field experiments for nitisol and ferralsols. The experimental results show a decrease in soil CLD content close to 70%. However, in the case of andosols, the efficiency of ISCR is only 25%. This lower efficiency of ISCR in andosols is not yet explained. Andosols represent around the half of the contaminated area in Martinique Island (Desprat et al. 2003) and consequently are important in terms of the whole contamination problem and the necessity to find remediation methods.

In the literature, the physical constraints of CLD availability to remediation process by microorganisms or reactive chemicals in soils, although mentioned as one of the factors that could limit CLD degradation (Macarie et al. 2016), have never been studied to our knowledge. However, the pore structure of soils is recognized as a critical factor in the sorption and entrapment of pesticides (Ahmad et al. 2004; Alexander 2000). The porous structure of the matrix with which pollutants are associated may influence the availability of the pollutant (Chung and Alexander 2002). In a previous study (Woignier et al. 2012), we have shown that the tortuous microstructure of the clay present in andosols affects the pesticide transfer from soil to crop, demonstrating a poor availability in these tropical soils.

In this paper, we investigate the influence of the physical features of soils (pore and aggregate size, microstructure, tortuosity) to pesticide bioavailability. The possibility to extract or transform the pesticides obviously depends on the possibility of interaction with a biological agent. That is to say that biological agent can access the pesticide molecules inside the porous structure, and/or that pesticide molecule can move

toward the biological agent. Each process is related to the difficulty for chemical or biological species to move and travel inside the porosity.

Thanks to structural models, we simulated the effect of pore size, microstructure, porosity, and tortuosity on transport properties (permeability and diffusion process) in volcanic soils.

The novelty of this study is to account for the impacts of some soil physical properties on the efficiency of eventual decontamination process. We expect that the soil microstructure in andosol will be a strong limitation to the proposed decontamination techniques.

We divided the paper into three parts. In the first part, we describe the main literature and results obtained on the effect of the type of soil on CLD retention and availability to biophysical processes. We propose that the physical properties of allophane clay likely affect the transfer process and pesticide accessibility. However, it is not possible to measure the transport properties at the scale (100 nm) of the clay aggregates. In the second part, we calculate the transport properties by two approaches: first, we simulate the tortuous microstructure of the allophane aggregates by numerical simulation with a “cluster–cluster aggregation model” (Kolb et al. 1983). Second, using a structural model (fractal approach), we calculate the evolution of some physical properties inside the clay aggregates. With these two methods, we study the relationship between, on the one hand, the allophane microstructure and, on the other hand, the tortuosity, the pore volume, and the associated permeability and diffusion at the nanometer scale. In the third part, we discuss how the literature and our simulation results could explain why these volcanic soils trap the pollutants and why these physical properties could render inefficient some of the actual decontamination methods proposed in the literature. We also propose an alternative to the decontamination: the pesticide sequestration.

## Materials and methods

### Soil samples

We sampled 45 soils at a depth of 0–20 cm near the “Montagne Pelée” volcano in Martinique (14° 40 N, 61° 00 W). Soils were andosols (allophane clay), nitisols (halloysite clay), and ferralsols (halloysite and Fe-oxihydroxides). We selected plots according to previous soil analyses to obtain a range of chlordecone concentrations that are representative of pollution in the FWI.

Organic carbon (C) contents were measured by dry combustion using a CHN chromatograph analyzer (Thermo

Finnigan Flash EA 1112, Thermo Finnigan Italia, Rodano, Italy).

Physical fractionation of soil was done by sieving in water (Bruckert et al. 1978), after soil dispersion in water and hexametaphosphate as previously described (Clostre et al. 2014b). We isolated three different organo mineral fractions: > 200  $\mu\text{m}$  size (a fraction), 50–200  $\mu\text{m}$  size (b fraction), and < 50  $\mu\text{m}$  size (c fraction). Three different samples of each kind of soil (andosol, nitisol, and ferralsol) were prepared in this way.

### CLD analysis

CLD content was measured at LDA26 (Valence, France), a laboratory accredited for pesticide analysis that works under norm NF17025. Extraction was carried out using dichloromethane and acetone (50:50 v/v) and CLD contents were measured in soils by gas chromatography coupled with tandem mass spectrometry (Varian MS 1200 triple quadrupole, Palo Alto, USA). Details of the techniques are given in the previous study by Cabidoche et al. (2009).

Leaching experiment was performed through water extraction to evaluate soil solution contamination by CLD (nine samples). Micro-columns containing 5 g of soil were prepared (four replicates for each soil). Leaching with 12.5 mL of nanopure water was slightly forced by gentle centrifugation (500g) directly in the micro-columns. Nanopure water was used to avoid CLD-contamination by tap water as described in Clostre et al. (2014b). The  $S/V$  ratio was around  $200\text{ cm}^{-1}$ , where  $S$  is the contact area and  $V$  is the liquid volume. After percolation through the soil columns, water CLD concentrations were determined. The soil-to-water transfer coefficient (WTC) is the ratio of the pesticide concentration in lixiviates to the pesticide concentration in soil expressed in  $\mu\text{g L}^{-1}/\mu\text{g kg}^{-1}$  of dry soil (Woignier et al. 2015).

### Drying procedure

The experimental techniques that give porous and structural information generally require dried solid samples. When andosols are dried, allophane clusters tend to shrink due to the increase in capillary stress within the pores as the pore water evaporates. As a result, the porous structure collapses, nanoscale porosity decreases, and specific surface area measurements give inconsistent results (Calvelo Pereira et al. 2019; Woignier et al. 2005). To preserve the porous and structural features of the soil samples, a critical point dryer (CPD 010, Balzers, Liechtenstein) was used. Liquid carbon dioxide ( $\text{CO}_2$ ) is suitable for the critical drying of soils because its critical point occurs at a temperature (31 °C) and pressure (7.4 MPa) that are readily attainable (Chevallier et al. 2010). The method, however, requires the use of an intermediate dehydrating agent (ethanol) that is miscible with both water

and liquid CO<sub>2</sub>. The soil samples were soaked for 24 h in absolute ethanol. The whole procedure was the same as that detailed in Woignier et al. (2005).

## Soil physical properties

The bulk density was calculated from the volume of soil samples (cylinders) and the weight of the soil samples dried in an oven (105 °C, 24 h). The pore volume was calculated from the bulk density and the solid density measured by He pycnometry. In the literature, the solid density is close to 2.5 g cm<sup>-3</sup> for the andosols, 2.66 g cm<sup>-3</sup> for the nitisols, and 2.6 for the ferralsols (Dorel et al. 2000; Biolders et al. 1990).

The mesopore features were characterized by N<sub>2</sub> adsorption techniques. Prior to N<sub>2</sub> adsorption, the outgassing conditions were 24 h at -196 °C using Micromeritics ASAP 2010 (SA, Verneuil-en-Halatte, France), with a 2–4-μm Hg vacuum. The specific surface area (*S*) was derived from 5-point adsorption isotherms in the relative pressure range between 0.05 and 0.30 by applying the Brunauer–Emmett–Teller (BET) equation (Brunauer et al. 1938). Pore size distribution (PSD) and cumulative mesopore volume (*V*<sub>meso</sub>) were calculated from desorption isotherms using the Barrett–Joyner–Halenda (BJH) model (Barrett et al. 1951). The soil powder was placed in a test tube and allowed to degas for 24 h at 50 °C in a vacuum of 2–4 μm Hg. The isotherms were measured by admitting or removing a known quantity of adsorbing gas into or out of the cell containing the sample maintained at a constant temperature of -196 °C.

The nanoscale structure was studied by small angle X-ray scattering (SAXS). The experiments were carried out on solid powders in 1 mm diameter glass capillaries. We worked in a transmission configuration and the whole procedure was the same as that detailed in Woignier et al. (2012).

Scattering techniques allow characterizing the nanostructure of allophane aggregates. In terms of fractal geometry, SAXS experiments provide different information on structure: the size of the fractal aggregates (*L*) and the compactness of the aggregates, which is characterized by the fractal dimension *D* (Marlière et al. 2001; Teixeira 1988).

The tortuosity inside the allophane aggregates is calculated from the fractal features; *t* is a power law function of the length scale:

$$t(l) \propto l^{\lambda-1} \quad (1)$$

$\lambda$  is the tortuosity exponent and can be derived from the fractal dimension (*D*) and the spreading dimension (*D*<sub>s</sub>) (Jullien and Botet 1987).

$$\lambda = D/D_s \quad (2)$$

$$\text{which leads to } t = l^{\lambda-1} a^{\lambda-1} \quad (3)$$

where *a* is the size of the allophane primary particles (*a* = 3–5 nm). Based on an analogy (Chevallier et al. 2008) between allophane and silica gels, we assume that the  $\lambda$  value is not very different from the exponent  $\lambda$  of nanoporous silica, between 1.4 and 1.8 (Courtens et al. 1987; Vacher et al. 1990). *t*, *D*, *D*<sub>s</sub>, and  $\lambda$  are dimensionless.

## Model approaches

The efficiency of a remediation technique is strongly dependent on the water and solute transport capacity in the soil microstructure and thus to the permeability and diffusion which control the traveling of chemical or biological species in the pore structure. Unfortunately, it is not possible to measure these properties at the scale of allophane aggregates (5–100 nm). To advance in this respect, model approaches are proposed hereafter.

The semiempirical Carman Kozeny equation describes the relationship between liquid permeability *K* and the porous features of a porous object (*V*<sub>p</sub>,  $\rho_s$ , and *S*) (Brinker and Scherer 1990; Carman 1937).

$$K = \rho_s V_p^3 / 5 (V_p \rho_s + 1) S^2 \quad (4)$$

Archie's law (Archie 1942) expresses the diffusion coefficient (*D*<sub>c</sub>) with the relative density ( $\rho/\rho_s$ ) and tortuosity (*t*) of the pore spaces. Diffusion along interstitial path with tortuosity *t* is reduced and gives:

$$D_c/D_{c0} = \left(1 - (\rho/\rho_s)/t^2\right) \quad (5)$$

where *D*<sub>c</sub> is the diffusion coefficient of diffusing species in the porous structure, and *D*<sub>c0</sub> is diffusion coefficient of diffusing species in the free liquid (Dullien and Brenner 1979).  $\rho$  and  $\rho_s$  are respectively the bulk and solid densities of the porous material. *D*<sub>c</sub>/*D*<sub>c0</sub>,  $\rho$ , and  $\rho_s$  are dimensionless.

## The cluster–cluster aggregation model

The cluster–cluster aggregation model quite satisfactorily describes typical structures of porous fractal systems obtained via particle aggregation, like silica gels and allophane aggregates (Primera et al. 2005; Woignier et al. 2006). In a previous work, we used a triangulation method in the pore space to calculate the pore size distribution of porous structure obtained by cluster–cluster aggregation. Details of the method are described elsewhere (Primera et al. 2003).

To build a porous microstructure, a set of *N* particles randomly place are allowed to undergo a Brownian diffusive motion, and irreversibly stick together with a probability *p* equal to 1 when they come into contact. Aggregates of particles are also able to diffuse and to stick to particles or to other aggregates. The procedure is repeated until all particles



aggregate. To calculate pore size distribution, we use a triangulation method in the pore space. The total pore space of the sample is measured by visiting the random points initially generated and placed in the void space of the sample. Details of the method are described elsewhere. Measuring the frequency of the appearance of a particular pore diameter yields the pore size distribution. The mean pore size of the simulated structure ( $D_{\text{num}}$ ) is extracted from the pore size distribution.

$$D_{\text{num}} = \sum_i f_i D_i / \sum_i f_i \quad (6)$$

where  $f_i$  is the frequency of appearance of pore diameter  $D_i$ . The porous surface  $S_{\text{num}}$  of the simulated porous systems is calculated as follows:

$$S_{\text{num}} = (\sum_{i=1}^N \sum_{j=1}^6 S_{ij}) / N \quad (7)$$

where  $j$  denotes the nearest neighbors of an occupied site  $i$  (6 in a cubic lattice),  $S_{ij} = 1$  if site  $j$  is empty, and  $S_{ij} = 0$  if not. Thus,  $S_{\text{num}}$  is the normalized number of free surfaces generated by the aggregation of the  $N$  particles. All numerical results reported in this work consist of a large average number of samples, never less than 50.

From the numerical pore size distribution, we calculate the simulated mean pore size  $D_{\text{sim}}$ , pore surface  $S_{\text{sim}}$ , and pore volume  $V_{\text{psim}}$  (Primera et al. 2005; Woignier et al. 2006). Data calculated by numerical simulation are dimensionless numbers; we then calculate the simulated features: simulated mean pore diameter  $D_{\text{sim}}$ , pore volume  $V_{\text{psim}}$ , and specific surface area  $S_{\text{sim}}$  from the results of simulation with Eqs. (8), (9), and (10).

$$D_{\text{sim}} = a D_{\text{num}} \quad (8)$$

$$S_{\text{sim}} = S_{\text{num}} / (\rho s a) \quad (9)$$

$$V_{\text{psim}} = D_{\text{num}} S_{\text{num}} / 4 \rho s \quad (10)$$

where  $a$  is the length of the elementary particle. Thanks to the simulated data, we can also calculate the permeability and diffusion coefficient of fractal aggregates using relations (4), (5), (9), and (10).

$$K = \rho s (D_{\text{num}} S_{\text{num}} / 4 \rho s)^3 / 5 ((D_{\text{num}} S_{\text{num}} / 4) + 1) (S_{\text{num}} / (\rho s a))^2 \quad (11)$$

$$Dc / Dc_0 = (V_{\text{psim}} \rho s - 1) / (V_{\text{psim}} \rho s) / t^2 \quad (12)$$

### Fractal approach

The fractal model allowed us to estimate changes in the transport properties inside the fractal microstructure.

The Carman Kozeny relation can be rewritten as (Brinker and Scherer 1990):

$$K \propto (1 - \rho / \rho s) d^2 \quad (13)$$

where  $d$  is the mean pore size. In the case of a hierarchical porous network, relative density is not a constant value but changes with the length scale.

$$\rho / \rho s (l) = (l/a)^{D-3} \quad (14)$$

$\rho / \rho s(l)$  expresses changes in the density inside the fractal aggregates for a length scale ranging between  $l$  and  $a$ ; where  $a$  is the size of the particles. In the case of allophane clay,  $a$  is close to 3–5 nm (Wada 1985; Chevallier et al. 2008).

With this model approach, the fractal structure gives an approximation of  $K$  at the aggregate scale  $l$  through the following equation.

$$K(l) \propto (1 - (l/a)^{D-3}) l^2. \quad (15)$$

The relations (5) and (14) allow a calculation of the diffusion coefficient inside the allophane aggregates through the following equation:

$$Dc(l) / Dc_0 \propto (1 - (l/a)^{D-3}) / t^2 \quad (16)$$

In a fractal aggregate, the tortuosity is also a power law function of the length scale:  $t(l) \propto l^{\lambda-1}$

$$Dc(l) / Dc_0 \propto (1 - (l/a)^{D-3}) / (l^{\lambda-1} a^{\lambda-1})^2 \quad (17)$$

These two model approaches, numerical simulation and fractal approach, show that the transport properties in soils strongly depend on the porous and textural features of the clay.

## Results

### Contamination of soil by chlordane

In this study, we fractionated nitisols, ferralsols, and andosols in 3 particle classes: size higher than 200  $\mu\text{m}$  (class a), between 50 and 200  $\mu\text{m}$  (class b), and lower than 50  $\mu\text{m}$  (class c). We then measured the CLD concentration (mg CLD/kg of dry soil) and relative concentration (%) for the different fractions a, b, and c (Table 1). In Table 1, “total” is the sum of a + b + c and a (%) is equal to a/total, b (%) is equal to b/total, and c (%) is equal to c/total.

For nitisol and ferralsol samples, the total CLD concentrations are quite homogeneous between 2.2 and 3.1  $\text{mg kg}^{-1}$ , showing small differences between a, b, and c fractions,

**Table 1** CLD concentration (mg CLD/kg of dry soil) and relative concentration (%) for the different fractions a, b, and c and porous characteristics: bulk density ( $\rho$ ), pore volume ( $V_p$ ), mesopore volume ( $V_{meso}$ ), and specific surface area ( $S$ ) of ferralsols, nitisols, and andosols

Soils	CLD in a	CLD in b	CLD in c	CLD total	CLD in a (%)	CLD in b (%)	CLD in c (%)	$\rho$ (g cm <sup>-3</sup> )	$V_p$ (cm <sup>3</sup> g <sup>-1</sup> )	$S$ (m <sup>2</sup> g <sup>-1</sup> )	$V_{meso}$ (cm <sup>3</sup> g <sup>-1</sup> )
Nitisol 1	0.681	1.140	0.956	2.777	24.5	41.1	34.4	0.89	0.75	46	0.17
Nitisol 2	0.660	0.990	0.950	2.600	25.4	38.1	36.5	0.87	0.77	78	0.16
Nitisol 3	0.947	1.214	0.777	2.938	32.2	41.3	26.4	1.00	0.62	43	0.15
Ferralsol 1	0.534	0.803	0.886	2.223	24.0	36.1	39.9	0.90	0.73	26	0.14
Ferralsol 2	0.751	1.013	1.017	2.781	27.0	36.4	36.6	0.86	0.79	78	0.19
Ferralsol 3	1.556	0.968	0.594	3.118	49.9	31	19.1	0.88	0.76	84	0.07
Andosol 1	1.155	2.388	6.209	9.752	11.8	24.5	63.7	0.60	1.26	109	0.36
Andosol 2	2.266	1.992	7.179	11.437	19.8	17.4	62.8	0.54	1.45	124	0.21
Andosol 3	1.160	2.140	10.250	13.550	8.6	15.8	75.6	0.76	0.91	85	0.28

accounting for 25 to 40% of the total contamination for the different relative class concentrations. In andosols, the total CLD content is in the range of 9.8–13.6 mg kg<sup>-1</sup> and the relative concentration clearly increases in the c fraction with 63 to 75% of the total CLD content retained in this fraction. These differences are because the c size class is rich in allophane aggregates (Filimonova et al. 2016). These results confirm the effect of the allophane content on the CLD retention in andosols (Brunet et al. 2009; Cabidoche et al. 2009).

Table 1 lists the porous characteristics of ferralsols, nitisols, and andosols. The main differences between the three different soils are the lower density, the higher specific surface area, and the larger mesoporous volume of andosol compared with nitisol and ferralsol. The data suggests that, in the case of andosols, a large part of the CLD is located in the mesoporous volume (1–100 nm). In the literature, authors explain that the structure of allophane aggregates is fractal and resembles a labyrinth at the 5–100 nm scale (Chevallier et al. 2008; Wada 1985). This description suggests that the accessibility in the allophane mesoporous volume is poor because of this nanomaterial structure.

In the following, we focus on andosols and allophane aggregates in such a way to discuss the specific impact of the allophane microstructure on remediation technique efficiency. The models that we develop in the “Model approaches” section necessitate structural and porous features like specific surface area, pore volume fractal features, aggregates size.... In the next section, we characterize the structure and porosity of allophane aggregates.

## Porous and structural features of allophane aggregates

To understand the influence of the clay nanostructure on pesticide bioavailability, we measure not only the structural features of the aggregates (aggregates size, fractal dimension, tortuosity...) but also the pore features (mesoporous volume, specific surface area) (Table 2). The N<sub>2</sub> adsorption curves allow calculating the pore size distribution of andosols. For the three andosols studied samples, the pores of the allophane aggregates are typically in the scale range of 5–100 nm. These results point to a hierarchical aggregation leading to a wide pore-size distribution (Chevallier et al. 2008). This description is in agreement with a qualitative fractal description. Electronic microscopy demonstrated that the clay aggregates (allophane) had a hierarchical microstructure (Adachi and

**Table 2** Porous and structural data of allophane aggregates from andosols

Physical characteristics	Symbol and unit	Data
Pore volume	$V_p$ (cm <sup>3</sup> g <sup>-1</sup> )	0.5–3
Mesoporous volume	$V_{meso}$ (cm <sup>3</sup> g <sup>-1</sup> )	0.05–0.4
Mesoporous range	$L_{meso}$ (nm)	5–100
Size of the fractal aggregates	$L$ (nm)	5–70
Size of allophane particles	$a$ (nm)	3–5
Fractal dimension	$D$	2.5–2.7
Specific surface area	$S$ (m <sup>2</sup> g <sup>-1</sup> )	50–200
Tortuosity	$t$	1.5–3.5

Karube 1999; Wada 1985; Woignier et al. 2015). The clay consists of aggregations of spherical allophane particles (see Fig. 1).

Table 2 lists the typical structural and porous features of allophane aggregates (Woignier et al. 2017). The fractal dimension  $D$  (2.5–2.7) and tortuosity  $t$  (1.5–3.5) are dimensionless.

As explained above, the allophane aggregate resembles a labyrinth at the nanometer scale. This description suggests that the accessibility inside the allophane aggregates decreases when the size of the labyrinth, the mesoporous porosity, and tortuosity increase. These conclusions are discussed later. In the following, we calculate the tortuosity and transport properties ( $t$ ,  $K$ , and  $D_c$ ) in allophane aggregates by numerical simulation and fractal models.

As explained above, we have no data concerning the transport properties like permeability, or diffusion in the mesoporous volume. To be able to extrapolate the transport properties in allophane aggregate, first we use a numerical model (cluster–cluster aggregation model (Kolb et al. 1983)). The  $D$  values are almost constant (2.5–2.7, Table 2), which means that the aggregation mechanism is quite the same, whatever the allophane concentration (5–25 allophane %). The measured  $D$  is rather close to the fractal dimension (2.2) corresponding to the “cluster–cluster aggregation” model (Kolb et al. 1983).

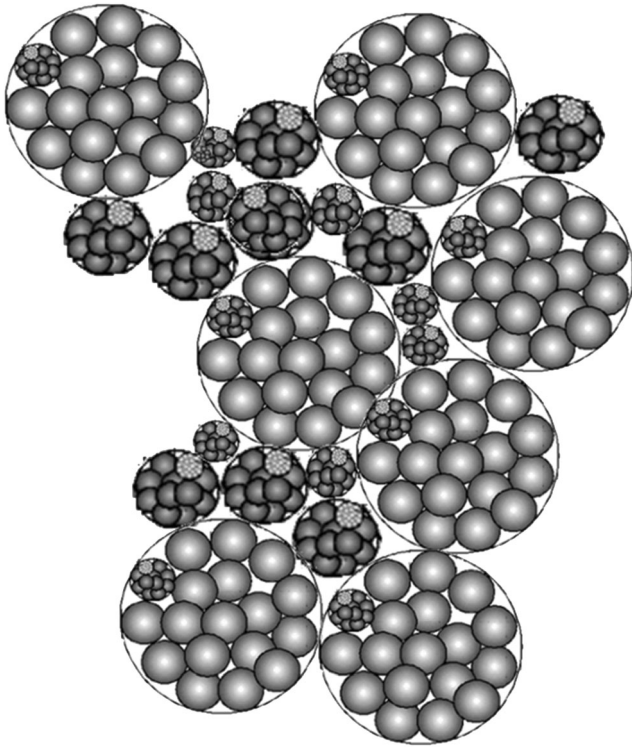


**Fig. 1** Schematic representation of fractal structure of allophane aggregates

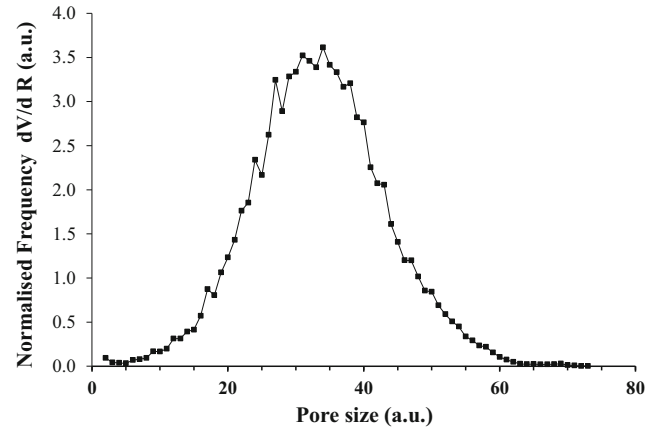


**Fig. 2** Numerical pores size distribution issued from cluster–cluster aggregation model

Figure 2 shows the pore size distribution issued from the numerical simulation. From the numerical pore size distribution and Eqs. (6), (7), and (8), we first calculate the numerical mean pore size  $D_{\text{num}}$ , pore surface  $S_{\text{num}}$ , and pore volume  $V_{\text{num}}$ , and we also derive the permeability and diffusion coefficient of fractal aggregates using relations (9) and (10). Table 3 summarizes the results of the porous properties calculated for allophane aggregates by numerical simulation.

It must be noted that the numerical model used (cluster–cluster aggregation model) to build the porous structure is characterized by a lower fractal dimension (2.2) than the measured  $D$  value (2.5). A lower fractal dimension means a more open structure with a larger pore volume and surface area. Thus, the comparison between Tables 2 and 3 shows that the numerical simulations are in a reasonable agreement with the range of the experimental value for  $S$  and  $V_p$ , although the numerical data are higher than the measured data (3–7 instead of 0.5–3  $\text{cm}^3 \text{g}^{-1}$  for  $V_p$  and 50–200 instead of 190–460  $\text{m}^2 \text{g}^{-1}$  for  $S$ ).

On the other hand, the calculated permeability in the range of 40–110  $\text{nm}^2$  is in good agreement with the permeability range of synthetic gels with a close fractal structure (Reynes et al. 2001; Scherer 1992). These two kinds of nanostructures (synthetic gels and allophane) have close features: pore volume, fractal structure, high tortuosity.... Allophane aggregates can be considered as natural minerals gels (Chevallier et al. 2008).

These simulated properties confirm that at the scale of the allophane aggregates, the tortuosity is high and the transport

**Table 3** Porous properties calculated for allophane aggregates by numerical simulation

$D_{\text{num}}$	$S_{\text{num}}$	$V_{\text{psim}}$	$D_{\text{sim}}$
21–31	1.5–3.5	3–7 $\text{cm}^3 \text{g}^{-1}$	63–93 nm
$S_{\text{sim}}$	$t$	$K$	$D_c/Dc_0$
190–460 $\text{m}^2 \text{g}^{-1}$	1.8–2.4	40–110 $\text{nm}^2$	0.15–0.21



properties ( $K$ ,  $D_c/D_{c0}$ ) are low. These “numerical” physical properties ( $t$ ,  $K$ ,  $D_c/D_{c0}$ ) give us a reasonable approximation of the mean properties of allophane aggregates. With the fractal model, we now calculate the physical properties inside the clay aggregates.

### Calculation of transport properties from fractal model

From fractal models, we calculated changes in  $K(l)$  versus the size of the clay with the relation (13) and  $D = 2.5$  and  $2.7$  (see Table 2). For this calculation, we considered that the value of the permeability outside of the allophane aggregate is quite close to the permeability calculated with the numerical model: around  $40\text{--}110\text{ nm}^2$  (Table 3).

Figure 3 shows that  $K(l)$  decreased markedly (more than a thousand fold) with a decrease of  $l$  between 100 and 5 nm, inside the aggregates. These results have the consequence that the liquid, with dissolved efficient chemical species, would not flow and would be trapped in the mesopores. In the literature, the  $t$  value for silica gels has been reported to range between 1.5 and 2.4 (Anez et al. 2014; Fosmoe and Hensch 1992; Woignier et al. 2018).

Figure 4 shows the diffusion coefficient ratio  $D_c/D_{c0}$  versus  $l$ , calculated with Eq. (13) for different values of tortuosity (1.5 and 2.4) and fractal dimension (2.5 and 2.7). This ratio strongly decreases in the fractal aggregate:  $D_c/D_{c0}$  can be as low as 0.01.

Figure 4 shows that  $D_c(l)/D_{c0}$  strongly decreases when pore size decreases from 100 to 4 nm and the diffusion coefficient in the fractal aggregates is around 100 times lower than in free liquid. The ratio  $D_c(l)/D_{c0}$  is much lower when the tortuosity increases which means that the diffusion in highly tortuous porous aggregates will be more difficult.

The calculations also demonstrate that  $K(l)$  and  $D_c(l)/D_{c0}$  decreased with an increase in the value of  $D$ . The higher  $D$  value is the signature of higher compactness resulting in lower flow and diffusion. Thus, the clay microstructure is highly

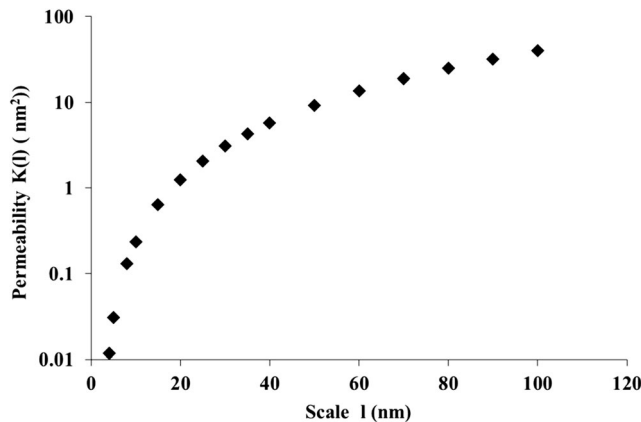


Fig. 3 Permeability  $K(l)$  versus the scale length ( $l$ ) calculated with relation (13) and  $D = 2.5$

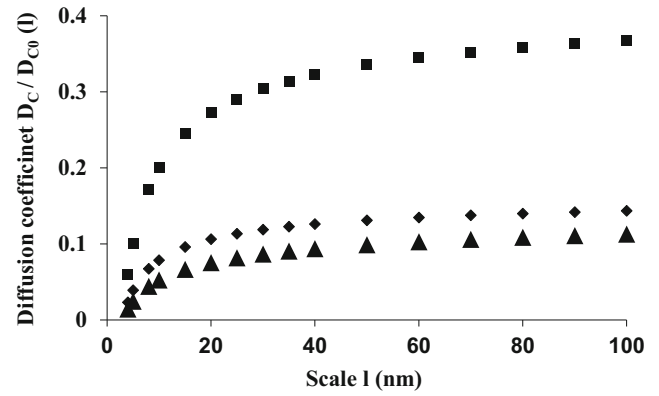


Fig. 4 Diffusion coefficient ratio  $D_c(l)/D_{c0}$  versus  $l$ , calculated with Eq. (15) for different values of tortuosity and fractal dimension  $t = 1.5$ ,  $D = 2.5$  (■);  $t = 2.4$ ,  $D = 2.5$  (◆); and  $t = 2.4$ ,  $D = 2.7$  (▲)

porous but has low transport properties ( $K(l)$  and  $D_c(l)/D_{c0}$ ) and fluids and chemical species migrate with difficulty inside the porosity.

These two model approaches, fractal and numerical simulation, show that the transport properties in soils strongly depend on the porous and textural features of the clay.

### Physical limits of the decontamination process

As explained above, 50% of contaminated soils are andosols (Desprat et al. 2003). Moreover, andosols are generally much more contaminated (CLD content 3–4 times higher) than the other type of contaminated soils (nitisols and ferralsols). Thus, we can say that andosols have to be at the center of soil decontamination concerns in FWI. In the following, we put forth the physical constraints for the decontamination of andosols.

The literature proposes the bioremediation to mineralize the pesticides by the action of bacteria or archaea in specific environmental conditions (anaerobic conditions). However, the size of bacteria and or archaea is typically in the range of the microns. Table 1 shows that a large part of the pesticide in andosols is stored in the allophane aggregates. From SAXS data, we have measured that,  $L$ , the size of the allophane aggregates is in the range of 5–100 nm. It is obvious that the pesticide molecules trapped in the allophane aggregates could never be directly accessible to bacteria nor archaea susceptible to mineralize the pesticides. Bacteria and archaea are clearly too large to migrate in the allophane aggregates. Bacteria or archaea actions could still take place by exudation, or external metabolism. Nevertheless, the physical constraint of CLD access will very likely considerably slow down the bioremediation kinetics.

Another promising approach to decontaminate is the ISCR (in situ chemical reduction) process. Recent works (Mouvet et al. 2016) on the three main types of FWI soils treated by ISCR have shown a reduction in the concentration of CLD and the formation of dechlorinated transformation products.

However, if ISCR seem to have a clear effect on studied nitisols and ferralsols with 70 to 75% of CLD transformation, this ratio drops to 25% in the case of andosols. As explained in the “Introduction” section, the ISCR method is based on the effect of the redox potential control by addition of Fe particles. Once again, the size of iron powder is around 50 microns, much larger than the allophane aggregates where a large part of CLD is retained. For andosols, the results of Table 1 show that around 24 to 38% of the pesticides are found in classes a and b of the fractionation experiment, it means that in soil aggregates, it is higher than 50 microns. Thus, only 25–40% of CLD will be directly accessible to the ISCR process and this would explain why only 25% of CLD was transformed. These simple steric considerations of size and accessibility could explain why the bioremediation or ISCR techniques are less efficient to fully decontaminate the andosols.

In summary, it is impossible for the ISCR or bioremediation techniques to be efficient at the scale of the allophane aggregate in andosols. However, we can suppose that, in the future, a “small enough” (lower than 100 nm) or dissolved chemical species could be able to transform CLD. In the following, we discuss the transport process inside the clay aggregates of such supposed chemical or biological species.

Results obtained by the fractal approach and the numerical simulation lead to the same conclusion: the transport properties inside the allophane aggregates are very poor, this mean that water and chemical or biological species will have difficulties flowing and diffusing inside the porosity of the fractal aggregates. In the same way, chlordecone molecule is trapped and may have the same difficulties to move toward biological species. All this reduces the likelihood of the chlordecone molecule meeting the chemical or biological species and so the bioavailability of the chlordecone. These approaches, modeling the composite structure of allophanic soils and calculating physical properties, could explain not only the poor pesticide availability in allophanic soils, but also the lower efficiency of the decontamination process in such soils. The pesticides stored in the vicinity or inside allophane aggregates are difficult to access and extract.

This conclusion is in qualitative agreement with the results in the literature (see sections 3.1) showing that soils containing allophane store large amounts of pollutants. The peculiar characteristics of the allophane structure (low pore size, tortuosity, and low transport properties) reduce the physical CLD accessibility to chemical or biological species.

This reduced accessibility is a strong constraint, which should be accounted for by future decontamination techniques, applied to andosols.

### Alternative techniques to decontamination

Because of the physical limitations described above, we concluded that we actually have no efficient method to

decontaminate andosols polluted by CLD. In any case, the allophane structure will be a physical constraint for a future remediation process. We thus propose an alternative to the complete decontamination, the pesticide sequestration.

Figure 5 shows the influence of the soil C content on the soil CLD content (andosols nitisols and ferralsols) and on the soil-to-water transfer coefficient of the pesticide (WTC). The figure shows that the chlordecone is retained in soils having a high C content (high CLD content and low water transfer coefficient). The higher the C content, the lower the CLD availability.

Soil amendments have been shown to influence soil pesticide processes like leaching and degradation (Cox et al. 2001; Thevenot et al. 2009). We have recently proposed an alternative to the complete decontamination (Clostre et al. 2014b; Woignier et al. 2013, 2016): the sequestration by the addition of compost. We showed that the addition of 5 wt% of compost strongly decreases the soil-to-water and to vegetables transfers of CLD (pot experiments). The chosen compost was a blend of sheepfold manure, fruit pulp and cake (olive, cacao, coffee, and sunflower), wool stuffing, and magnesium, with 47% organic content. We tested the effect of organic matter addition on plant transfer and we compared soil to crop transfers of chlordecone with and without compost incorporation. Transfers were calculated as the ratio of chlordecone content in the plant sample ( $\mu\text{g kg}^{-1}$  fresh weight) to soil chlordecone content ( $\mu\text{g kg}^{-1}$  dry soil) and normalized to transfer in control soil.

Adding the organic amendment significantly reduced soil-to-plant transfer by a factor of fifteen for radish, a factor of four for lettuce, and a factor of 2 for cucumber (pot experiments) (Woignier et al. 2013). In field conditions, organic amendment significantly reduced transfer to plant organs for

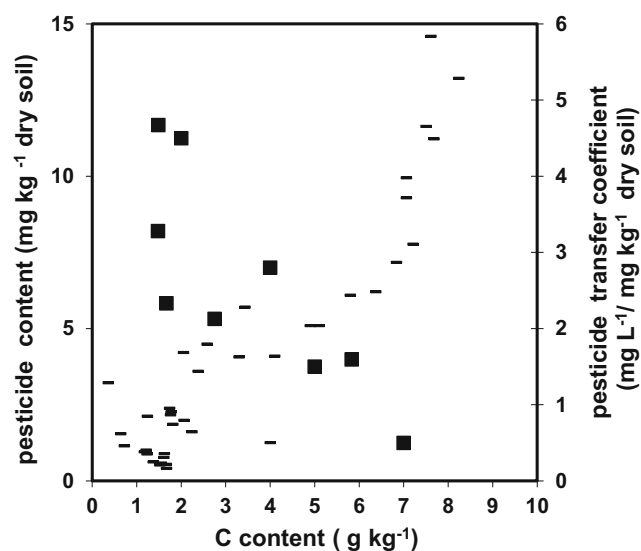


Fig. 5 Soil chlordecone content (■) and pesticide transfer coefficient (---) versus soil C content

radish, cucumber, and sweet potatoes crops (Clostre et al. 2014b). Results showed a lesser plant uptake with organic amendment; uptake was divided respectively by four, three, and two for radish, cucumber, and sweet potato, 6 months after compost addition.

## Conclusion

In Martinique, the chlordecone soil pollution is the contamination source for crops and water resources as well as farm animals and aquatic food resources. Andosols are the most contaminated soils and represent around 50% of the contaminated area. Andosols contain short-range nanoclays (allophane) fractal aggregates with high tortuosity. Taking into account the small size porosity of allophane aggregates (100 nm) which traps the CLD in andosols, bacteria or chemical process actually proposed in the literature could not directly access to the allophane porosity and be fully efficient to decontaminate andosols.

With numerical simulation and fractal models, we showed that, at the scale of the aggregates, the calculated transport properties are very low because of the allophane microstructure. This property represents a challenge for soil CLD remediation because it asks for the physical accessibility of extraction processes. The reduced accessibility in allophane clay will control the efficiency of proposed decontamination techniques leading to the conclusion that andosols will be very difficult to fully decontaminate. The chemical affinity of CLD for organic matter allowed us to propose an alternative to decontamination: the pesticide sequestration by compost addition.

**Acknowledgments** Many thanks to Dr Hervé Macarie for helpful discussions.

**Funding information** Our work has been funded by the Chlordecone National Action Plan, the European FEDER funds of Martinique, and the France-Venezuela PCP program (“Matériaux Nanostructurés pour un développement durable” project).

## Compliance with ethical standards

**Conflict of interest** The authors declare that they have no conflict of interest.

## References

- Adachi Y, Karube J (1999) Application of a scaling law to the analysis of allophane aggregates. *Colloids Surf A Physicochem Eng Asp* 151(1-2):43–47
- Ahmad R, Kookana RS, Megharaj M, Alston AM (2004) Aging reduces the bioavailability of even a weakly sorbed pesticide (carbaryl) in soil. *Environ Toxicol Chem* 23(9):2084–2089. <https://doi.org/10.1897/03-569>
- Alexander M (2000) Aging, bioavailability, and overestimation of risk from environmental pollutants. *Environ Sci Technol* 34(20):4259–4265. <https://doi.org/10.1021/es001069+>
- Anez L, Calas-Etienne S, Primera J, Woignier T (2014) Gas and liquid permeability in nano composites gels: comparison of Knudsen and Klinkenberg correction factors. *Microporous Mesoporous Mater* 200:79–85. <https://doi.org/10.1016/j.micromeso.2014.07.049>
- Archie GE (1942) The electrical resistivity log as an aid in determining some reservoir characteristics. *Trans Am Inst Min Metall Pet Eng* 146(01):54–62. <https://doi.org/10.2118/942054-G>
- ATSDR (1995) Mirex and chlordecone. [www.atsdr.cdc.gov/toxprofiles/tp66.pdf](http://www.atsdr.cdc.gov/toxprofiles/tp66.pdf). Accessed May 2019
- Barrett EP, Joyner LG, Halenda PP (1951) The determination of pore volume and area distributions in porous substances. I. Computations from nitrogen isotherms. *J Am Chem Soc* 73(1): 373–380
- Bielders CL, De Backer LW, Delvaux B (1990) Particle density of volcanic soils as measured with a gas pycnometer. *Soil Sci Soc Am J* 54(3):822–826. <https://doi.org/10.2136/sssaj1990.03615995005400030034x>
- Brinker CJ, Scherer GW (1990) *Sol-gel science: the physics and chemistry of sol-gel processing*. Academic, London
- Bruckert S, Andreux F, Correa A, Ambouta K, Souchier B (1978) Fractionnement des agrégats appliqué à l'analyse des complexes organominéraux des sols. In: AISS (ed) *Comptes-Rendus du 11ème Congrès International de Science du Sol*, Edmonton, Canada, pp 88–89
- Brunauer S, Emmett PH, Teller E (1938) Adsorption of gases in multimolecular layers. *J Am Chem Soc* 60(2):309–319. <https://doi.org/10.1021/ja01269a023>
- Brunet D, Woignier T, Lesueur-Jannoyer M, Achard R, Rangon L, Barthès BG (2009) Determination of soil content in chlordecone (organochlorine pesticide) using near infrared reflectance spectroscopy (NIRS). *Environ Pollut* 157(11):3120–3125. <https://doi.org/10.1016/j.envpol.2009.05.026>
- Cabidoche YM, Lesueur-Jannoyer M (2012) Contamination of harvested organs in root crops grown on chlordecone-polluted soils. *Pedosphere* 22(4):562–571. [https://doi.org/10.1016/s1002-0160\(12\)60041-1](https://doi.org/10.1016/s1002-0160(12)60041-1)
- Cabidoche YM, Achard R, Cattani P, Clermont-Dauphin C, Massat F, Sansoulet J (2009) Long-term pollution by chlordecone of tropical volcanic soils in the French West Indies: a simple leaching model accounts for current residue. *Environ Pollut* 157(5):1697–1705. <https://doi.org/10.1016/j.envpol.2008.12.015>
- Calabi-Floody M, Bendall JS, Jara AA, Welland ME, Theng BKG, Rumpel C, de la Luz Mora M (2011) Nanoclays from an andisol: extraction, properties and carbon stabilization. *Geoderma* 161(3–4): 159–167. <https://doi.org/10.1016/j.geoderma.2010.12.013>
- Calvelo Pereira R, Camps Arbestain M, Kelliher FM, Theng BKG, McNally SR, Macías F, Guitián F (2019) Assessing the pore structure and surface area of allophane-rich and non-allophanic topsoils by supercritical drying and chemical treatment. *Geoderma* 337:805–811. <https://doi.org/10.1016/j.geoderma.2018.10.037>
- Carman PC (1937) Fluid flow through granular beds. *Trans Inst Chem Eng* 15:150–166
- Chevallier T, Woignier T, Toucet J, Blanchart E, Dieudonné P (2008) Fractal structure in natural gels: effect on carbon sequestration in volcanic soils. *J Sol-Gel Sci Technol* 48(1):231–238. <https://doi.org/10.1007/s10971-008-1795-z>
- Chevallier T, Woignier T, Toucet J, Blanchart E (2010) Organic carbon stabilization in the fractal pore structure of andosols. *Geoderma* 159(1–2):182–188
- Chevallier M, Della-Negra O, Chaussonnerie S, Barbance A, Muselet D, Lagarde F, Darii E, Ugarte E, Lescop E, Fonknechten N,

- Weissenbach J, Woignier T, Gallard J, Vuilleumier S, Imfeld G, Le Paslier D, Saaïdi P (2019) Natural chlordecone degradation revealed by numerous transformation products characterized in key French West Indies environmental compartments. *Environ Sci Technol* 53(11):6133–6143. <https://doi.org/10.1021/acs.est.8b06305>
- Chung N, Alexander M (2002) Effect of soil properties on bioavailability and extractability of phenanthrene and atrazine sequestered in soil. *Chemosphere* 48(1):109–115. [https://doi.org/10.1016/s0045-6535\(02\)00045-0](https://doi.org/10.1016/s0045-6535(02)00045-0)
- Clostre F, Lesueur-Jannoyer M, Achard R, Letourmy P, Cabidoche Y-M, Cattani P (2014a) Decision support tool for soil sampling of heterogeneous pesticide (chlordecone) pollution. *Environ Sci Pollut Res* 21(3):1980–1992. <https://doi.org/10.1007/s11356-013-2095-x> (In English)
- Clostre F, Woignier T, Rangan L, Fernandes P, Soler A, Lesueur-Jannoyer M (2014b) Field validation of chlordecone soil sequestration by organic matter addition. *J Soils Sediments* 14(1):23–33. <https://doi.org/10.1007/s11368-013-0790-3>
- Clostre F, Letourmy P, Lesueur-Jannoyer M (2017) Soil thresholds and a decision tool to manage food safety of crops grown in chlordecone polluted soil in the French West Indies. *Environ Pollut* 223:357–366. <https://doi.org/10.1016/j.envpol.2017.01.032>
- Coat S, Monti D, Legendre P, Bouchon C, Massat F, Lepoint G (2011) Organochlorine pollution in tropical rivers (Guadeloupe): role of ecological factors in food web bioaccumulation. *Environ Pollut* 159(6):1692–1701. <https://doi.org/10.1016/j.envpol.2011.02.036>
- Courtens E, Pelous J, Phalippou J, Vacher R, Woignier T (1987) Brillouin-scattering measurements of phonon-fracton crossover in silica aerogels. *Phys Rev Lett* 58(2):128–131
- Cox L, Cecchi A, Celis R, Hermosín MC, Koskinen WC, Cornejo J (2001) Effect of exogenous carbon on movement of simazine and 2,4-D in soils. *Soil Sci Soc Am J* 65(6):1688–1695. <https://doi.org/10.2136/sssaj2001.1688>
- Dallaire R, Muckle G, Rouget F, Kadhel P, Bataille H, Guldner L, Seurin S, Chajès V, Monfort C, Boucher O, Pierre Thomé J, Jacobson SW, Multigner L, Cordier S (2012) Cognitive, visual, and motor development of 7-month-old Guadeloupean infants exposed to chlordecone. *Environ Res* 118:79–85. <https://doi.org/10.1016/j.envres.2012.07.006>
- Dawson GW, Weimer WC, Shupe SJ (1979) Kepone – a case study of a persistent material. *Am Inst Chem Eng Symposium Series* 75:366–374
- Della Rossa P, Jannoyer M, Mottes C, Plet J, Bazizi A, Arnaud L, Jestin A, Woignier T, Gaude J-M, Cattani P (2017) Linking current river pollution to historical pesticide use: insights for territorial management? *Sci Total Environ* 574:1232–1242. <https://doi.org/10.1016/j.scitotenv.2016.07.065>
- Desprat JF, Comte JP, Perrian G (2003) Cartographie par analyse multicritère des sols potentiellement pollués par organochlorés en Martinique, Rapport phase 2 BRGM RP 52257 (in French) <http://infoterre.brgm.fr/rapports/RP-52257-FR.pdf>. Accessed 2003
- Dolfing J, Novak I, Archelas A, Macarie H (2012) Gibbs free energy of formation of chlordecone and potential degradation products: implications for remediation strategies and environmental fate. *Environ Sci Technol* 46(15):8131–8139. <https://doi.org/10.1021/es301165p>
- Dorel M, Roger-Estrade J, Manichon H, Delvaux B (2000) Porosity and soil water properties of Caribbean volcanic ash soils. *Soil Use Manag* 16(2):133–140
- Dubuisson C, Héraud F, Leblanc J-C, Gallotti S, Flamand C, Bateau A, Quenel P, Volatier J-L (2007) Impact of subsistence production on the management options to reduce the food exposure of the Martinican population to Chlordecone. *Regul Toxicol Pharmacol* 49(1):5–16. <https://doi.org/10.1016/j.yrtph.2007.04.008>
- Dullien FAL, Brenner H (1979) Porous media: fluid transport and pore structure. Academic, Cambridge
- Durimel A, Altenor S, Miranda-Quintana R, Couespel Du Mesni P, Jauregui-Haza U, Gadiou R, Gaspard S (2013) pH dependence of chlordecone adsorption on activated carbons and role of adsorbent physico-chemical properties. *Chem Eng J* 229:239–249
- Epstein SS (1978) Kepone-Hazard evaluation. *Sci Total Environ* 9(1):1–62. [https://doi.org/10.1016/0048-9697\(78\)90002-5](https://doi.org/10.1016/0048-9697(78)90002-5)
- Filimonova S, Kaufhold S, Wagner FE, Häusler W, Kögel-Knabner I (2016) The role of allophane nano-structure and Fe oxide speciation for hosting soil organic matter in an allophanic Andosol. *Geochim Cosmochim Acta* 180:284–302. <https://doi.org/10.1016/j.gca.2016.02.033>
- Fosmoe A, Hench LL (1992) Gas permeability in porous gel-silica. In: LL Hench JKW (ed) Chemical processing of advanced materials. Wiley, New York, pp 897–905
- Garrido-Ramirez EG, Sivaiah MV, Barrault J, Valange S, Theng BKG, Ureta-Zañartu MS, Mora ML (2012) Catalytic wet peroxide oxidation of phenol over iron or copper oxide-supported allophane clay materials: influence of catalyst SiO<sub>2</sub>/Al<sub>2</sub>O<sub>3</sub> ratio. *Microporous Mesoporous Mater* 162:189–198. <https://doi.org/10.1016/j.micromeso.2012.06.038>
- Gaspard S, Ranguin R, Jaurégui Haza U, Passé-Coutin N, Durimel A (2016) Remediation of chlordecone contaminated waters using activated carbons chap 16. In: Lesueur Jannoyer M, Cattani P, Woignier T, Clostre F (eds) Crisis management of chronic pollution: contaminated soil and human health. Urbanization, industrialization and the environment. CRC Press, Boca Raton, pp 223–236
- Irwin Abbey AM, Beaudette LA, Lee H, Trevors JT (2003) Polychlorinated biphenyl (PCB) degradation and persistence of a gfp-marked *Ralstonia eutropha* H850 in PCB-contaminated soil. *Appl Microbiol Biotechnol* 63(2):222–230. <https://doi.org/10.1007/s00253-003-1380-x>
- Jondreville C, Lavigne A, Clostre F, Jurjanz S, Dalibard C, Liabeuf J-M, Lesueur-Jannoyer M (2013) Contamination of grazing ducks by chlordecone in Martinique. In: EAAP - 64th Annual Meeting, Nantes, France. Book of abstract. Wageningen Academic Publishers, pp 166–166
- Jullien R, Botet R (1987) Aggregation and fractal aggregates. World Scientific, Singapore
- Kim S-C, Yang JE, Ok YS, Skousen J, Kim D-G, Joo J-H (2010) Accelerated metolachlor degradation in soil by zerovalent iron and compost amendments. *Bull Environ Contam Toxicol* 84(4):459–464. <https://doi.org/10.1007/s00128-010-9963-6>
- Kolb M, Botet R, Jullien R (1983) Scaling of kinetically growing clusters. *Phys Rev Lett* 51(13):1123–1126
- Lesueur Jannoyer M, Cattani P, Woignier T, Clostre F (eds) (2016) Crisis management of chronic pollution: contaminated soil and human health, Urbanization, industrialization and the environment series, vol, vol 2. CRC Press, Boca Raton États-Unis (In eng)
- Levillain J, Cattani P, Colin F, Voltz M, Cabidoche Y-M (2012) Analysis of environmental and farming factors of soil contamination by a persistent organic pollutant, chlordecone, in a banana production area of French West Indies. *Agric Ecosyst Environ* 159:123–132. <https://doi.org/10.1016/j.agee.2012.07.005>
- Liber Y, Létondor C, Pascal-Lorber S, Laurent F (2018) Growth parameters influencing uptake of chlordecone by *Miscanthus* species. *Sci Total Environ* 624:831–837
- Liu C, Li H, Teppen BJ, Johnston CT, Boyd SA (2009) Mechanisms associated with the high adsorption of dibenzo-p-dioxin from water by smectite clays. *Environ Sci Technol* 43(8):2777–2783. <https://doi.org/10.1021/es802381z>
- Macarie H, Novac I, Sastre-Conde I, Labrousse Y, Archelas A, Dolfing J (2016) Theoretical approach to chlordecone remediation. Chap 14. In: Lesueur Jannoyer M, Cattani P, Woignier T, Clostre F (eds) Crisis management of chronic pollution: contaminated soil and human health. Urbanization, industrialization and the environment. CRC Press, Boca Raton, pp 191–209



- Marlière C, Woignier T, Dieudonné P, Primera J, Lamy M, Phalippou J (2001) Two fractal structures in aerogel. *J Non-Cryst Solids* 285: 175–180. [https://doi.org/10.1016/S0022-3093\(01\)00450-1](https://doi.org/10.1016/S0022-3093(01)00450-1)
- Mottes C, Charlier J-B, Rocle N, Gresser J, Lesueur-Jannoyer M, Cattani P (2016) Chlordecone case study in the French West Indies. In: Lesueur Jannoyer M, Cattani P, Woignier T, Clostre F (eds) *Crisis management of chronic pollution: contaminated soil and human health. Urbanization, industrialization and the environment*. CRC Press, Boca Raton, pp 121–130
- Mottes C, Lesueur Jannoyer M, Le Bail M, Guéné M, Carles C, Malézieux E (2017) Relationships between past and present pesticide applications and pollution at a watershed outlet: the case of a horticultural catchment in Martinique, French West Indies. *Chemosphere* 184:762–773. <https://doi.org/10.1016/j.chemosphere.2017.06.061>
- Mouvet C, Dictor M-C, Bristeau S, Breeze D, Mercier A (2016) Remediation by chemical reduction in laboratory mesocosms of three chlordecone-contaminated tropical soils. *Environ Sci Pollut Res*:1–13. <https://doi.org/10.1007/s11356-016-7582-4>
- Multigner L, Ndong JR, Giusti A (2010) Chlordecone exposure and risk of prostate cancer. *J Clin Oncol* 28:3457–3462
- Peters R, Kelsey JW, White JC (2007) Differences in p,p'-DDE bioaccumulation from compost and soil by the plants *Cucurbita pepo* and *Cucurbita maxima* and the earthworms *Eisenia fetida* and *Lumbricus terrestris*. *Environ Pollut* 148(2):539–545. <https://doi.org/10.1016/j.envpol.2006.11.030>
- Phillips TM, Lee H, Trevors JT, Seech AG (2006) Full-scale in situ bioremediation of hexachlorocyclohexane-contaminated soil. *J Chem Technol Biotechnol* 81(3):289–298. <https://doi.org/10.1002/jctb.1390>
- Pignatello JJ (1998) Soil organic matter as a nanoporous sorbent of organic pollutants. *Adv Colloid Interface Sci* 76–77:445–467. [https://doi.org/10.1016/S0001-8686\(98\)00055-4](https://doi.org/10.1016/S0001-8686(98)00055-4)
- Primera J, Hasmy A, Woignier T (2003) Numerical study of pore sizes distribution in gels. *J Sol-Gel Sci Technol* 26(1-3):671–675. <https://doi.org/10.1023/A:1020765230983> (In English)
- Primera J, Woignier T, Hasmy A (2005) Pore structure simulation of gels with a binary monomer size distribution. *J Sol-Gel Sci Technol* 34(3):273–280. <https://doi.org/10.1007/s10971-005-2524-5> (In English)
- Reynes J, Woignier T, Phalippou J (2001) Permeability measurement in composite aerogels: application to nuclear waste storage. *J Non-Cryst Solids* 285(1–3):323–327. [https://doi.org/10.1016/S0022-3093\(01\)00474-4](https://doi.org/10.1016/S0022-3093(01)00474-4)
- Scherer GW (1992) Bending of gel beams: method for characterizing elastic properties and permeability. *J Non-Cryst Solids* 142:18–35. [https://doi.org/10.1016/S0022-3093\(05\)80003-1](https://doi.org/10.1016/S0022-3093(05)80003-1)
- Seech A, Bolanos-Shaw K, Hill D, Molin J (2008) In situ bioremediation of pesticides in soil and groundwater. *Remediation* 19(1):87–98. <https://doi.org/10.1002/rem.20193>
- Semple KT, Reid BJ, Fermor TR (2001) Impact of composting strategies on the treatment of soils contaminated with organic pollutants. *Environ Pollut* 112(2):269–283. [https://doi.org/10.1016/S0269-7491\(00\)00099-3](https://doi.org/10.1016/S0269-7491(00)00099-3)
- Teixeira J (1988) Small angle scattering by fractal systems. *J Appl Crystallogr* 21:781–785
- Thevenot M, Dousset S, Hertkorn N, Schmitt-Kopplin P, Andreux F (2009) Interactions of diuron with dissolved organic matter from organic amendments. *Sci Total Environ* 407(14):4297–4302. <https://doi.org/10.1016/j.scitotenv.2009.04.021>
- UNEP (2007) Report of the persistent organic pollutants review committee on the work of its third meeting. Addendum. Risk management evaluation on chlordecone. Geneva, Switzerland
- Vacher R, Courtens E, Coddens G, Heidemann A, Tsujimi Y, Pelous J, Foret M (1990) Crossovers in the density of states of fractal silica aerogels. *Phys Rev Lett* 65(8):1008–1011
- Wada K (1985) The distinctive properties of Andosol. *Adv Soil Sci* 2: 173–229
- Woignier T, Braudeau E, Doumenc H, Rangon L (2005) Supercritical drying applied to natural “gels”: allophanic soils. *J Sol-Gel Sci Technol* 36(1):61–68. <https://doi.org/10.1007/s10971-005-2659-4>
- Woignier T, Primera J, Hashmy A (2006) Application of the DLCA model to natural gels: the allophanic soils. *J Sol-Gel Sci Technol* 40(2-3):201–207. <https://doi.org/10.1007/s10971-006-7593-6>
- Woignier T, Clostre F, Macarie H, Jannoyer M (2012) Chlordecone retention in the fractal structure of volcanic clay. *J Hazard Mater* 241–242:224–230. <https://doi.org/10.1016/j.jhazmat.2012.09.034>
- Woignier T, Fernandes P, Soler A, Clostre F, Carles C, Rangon L, Lesueur-Jannoyer M (2013) Soil microstructure and organic matter: keys for chlordecone sequestration. *J Hazard Mater* 262:357–364. <https://doi.org/10.1016/j.jhazmat.2013.08.070>
- Woignier T, Duffours L, Colombel P, Dieudonné P (2015) Nanoporous clay with carbon sink and pesticide trapping properties. *Eur Phys J Special Topics* 224:1945–1962. <https://doi.org/10.1140/epjst/e2015-02512-x>
- Woignier T, Clostre F, Fernandes P, Rangon L, Soler A, Lesueur-Jannoyer M (2016) Compost addition reduces porosity and chlordecone transfer in soil microstructure. *Environ Sci Pollut Res* 23(1):98–108. <https://doi.org/10.1007/s11356-015-5111-5>
- Woignier T, Clostre F, Fernandes P, Soler A, Rangon L, Sastre-Conde MI, Jannoyer ML (2017) The pesticide chlordecone is trapped in the tortuous mesoporosity of allophane clays. *Environ Sci Pollut Res*: 1–12. <https://doi.org/10.1007/s11356-017-9370-1>
- Woignier T, Anez L, Calas-Etienne S, Primera J (2018) Gas slippage in fractal porous material. *J Nat Gas Sci Eng* 57:11–20. <https://doi.org/10.1016/j.jngse.2018.06.043>